

DART TILT ROTOR PROGRAM MANUFACTURING AND TESTS STATUS

Ester Porras	Henri De Vries	Markus Bauer	Mathieu Da-Rold	Felice De Nicola	Zoppitelli ¹
SPASA	NLR	EUROCOPTER	PAULSTRA	CIRA	EUROCOPTER

Abstract

Since June 2004, after 27 months of specification and detailed design activities which led to the drawings freeze, the DART program has entered the manufacturing phase. Due to the great variety of parts manufacturing levels of complexity, the parts delivery have spanned over a period of 12 months. This paper presents the DART program manufacturing activities with details on the technologies developed by the partners of the consortium. It also presents some preliminary tests results on some parts as well as on some subsystems.

The DART tilt-rotor project is one of the 6 Critical Technology Projects partly funded by the European Commission that are related to the TILT-ROTOR. It is oriented towards the design and manufacturing of a full-scale rotor hub for an advanced European Tilt-Rotor configuration called ERICA (Enhanced Rotorcraft Innovative Concept Achievement). Details on the program can be found on reference [21].

The paper first presents the manufacturing activity. It describes the processes used for the main metallic parts, such as the hub-spring frames, the combiner. It then covers the details of some major composite hub components manufacturing, including mould designs and curing cycles definition. This section ends with a presentation of the manufacturing of the elastomeric parts, and more particularly the hub-spring, the centrifugal force pitch bearing, and the homokinetic drive system bearing.

It then covers the tests that took place or are presently being conducted at PAULSTRA and EC facilities. They include the elastomeric parts tests, the spindle test, the homokinetic drive system test, and the complete hub static test. Some tests are characterization tests while others are fatigue tests. For the centrifugal force bearing test, a specific buckling test was also performed.

[1] Rotors design – DART technical manager.

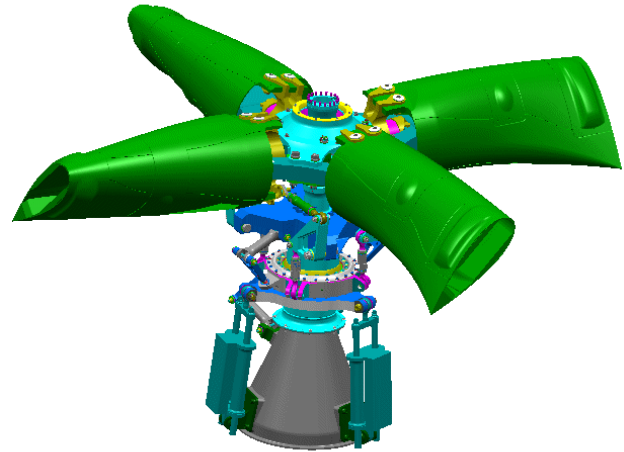


Figure 1: The DART rotor

Introduction

DART is one of the 6 Critical Technology Projects , partially funded by the European Commission, that were submitted under Key Action “New perspective in Aeronautics” promoting the programme of Competitive and Sustainable Growth in the 5th Framework programme.

These projects are respectively:

- DART, for the design, manufacturing and testing of a full-scale hub,
- RHILP and ACT-TILT, oriented towards the study of the Flight Control System and handling qualities,
- TILTAERO, mainly for the study of interactional aerodynamics at low speed,
- ADYN, with the purpose of investigating dynamics and acoustic aspects, and
- TRISYD, focused on the development of the drive system.

The DART rotor stringent requirements in terms of safety, weight, cost, and performance have led to the

development of innovative designs and manufacturing concepts.

It is well known that composites help achieve important weight and costs savings, in addition to better fail-safe properties. For these reasons, they were chosen for two major components: the cuff and the yoke, each of them presenting particular challenges.

The choice of elastomeric bearings was dictated by the clear advantages they provide in terms of on-condition maintenance, lubrication-free and fail safe characteristics. For the particular tilt rotor application, the development of the pitch bearings, the homokinetic drive system, and hub-spring bearings presented important challenges due to the large pitch range and self-heating properties.

Although more classical, the manufacturing of metallic components involved a tight planning control. This was necessary to guarantee early delivery of parts which were used for anticipated testing. Likewise, the elastomeric frames had to be delivered early because these parts required additional time for moulding and testing.

The tests are organised into samples, components, and systems testing.

The samples testing was limited to the pre-preg used for the yoke. Several tests were performed for various curing parameters in order to confirm the good fatigue properties of the material that were expected after the curing cycle optimisation.

The components testing were limited to the elastomeric bearings. They included characterization tests that are used as input for aero elastic investigation and fatigue tests to predict reliability. For the centrifugal force pitch bearing, the large pitch excursions requirements have led to a design with a large number of shims and which may be subject to a buckling type of instability. To assess this risk, a specific test was performed.

The systems testing were limited to the critical components of the DART hub:

- the spindle – bearing attachment
- the homokinetic drive system
- the complete hub

The systems tests have been performed to assess the global behaviour of the system: capacity to withstand loads, loads sharing, and global stiffness properties.

Manufacturing

Metallic components

SPASA and EUROCOPTER were the major contributors to the manufacturing of metallic components. SPASA is a Spanish SME dedicated to high precision metal machining. Its main role in the DART project has been for parts of the rotating control system and the frames of the elastomeric components. It is certified according to EN9100 standard.

Typically, the production process of these parts involves the following steps:

Material procurement: despite the tight planning, and reduced quantities that have added difficulties and increased costs to the program, all parts materials have been ordered in time.



Figure 2: CF Bearing Frame. SPASA photo

Manufacturing: This activity ranges from tools design up to machining, usually requiring different techniques (turning, milling, broaching, etc) and intermediate surface treatments and/or assemblies. This is the case of the hub-spring outer frames for which some finishing operations were performed after bushes installation in order to ensure tight positions tolerances.



Figure 3: Hub spring frame. SPASA photo

The tight tolerances required for DART parts production can be highlighted as a general difficulty found during manufacturing.

As a particular and difficult case, the broaching process for producing the inner part of the lower and the upper hub spring frames required a very large tooling (1,5 m long). This is quite unusual and was the consequence of the large diameter to reach. This fact generated serious difficulties not just for the process execution but for the quality requirements fulfilment.

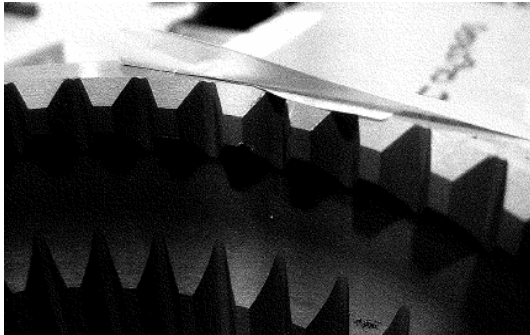


Figure 4: Detail of the broached operation in the Inner upper Hub Spring frame. SPASA photo

Dimensional verification: all parts were controlled after each manufacturing operation to ensure the part fulfils the requirements or to allow the launch of the required repair actions. Most of the dimensional verifications were performed in the 3D measurer of SPASA (DEA) and full dimensional reports were added to the individual parts documentation.

SPASA quality department performed the required inspections after dimensional verification informing about all non-compliances which occurred during machining.

Surface and final treatments: they were required for all parts and no specific difficulties were found except for those parts requiring very local hard chromic anodising as well as tight tolerances. The parts affected by this treatment were the outer hub spring frames.

Quality inspections: they were performed after final treatments following the already mentioned procedure of documentation and delivery of non compliances information when required

Assembly: most of the parts manufactured by SPASA required assembly operations, usually bushes installation. In most cases, bushes installation was done through interference fit using parts cooling in liquid nitrogen. Previous tests during design phase had to be performed in order to define

the dimensions and tolerances of the involved parts to ensure the right installation by using this method.



Figure 5: Detail of Outer hub spring frame. SPASA photo

For some parts, very specific and precise tooling was required to ensure correct installation of bushings, in particular, those of the combiner plate.

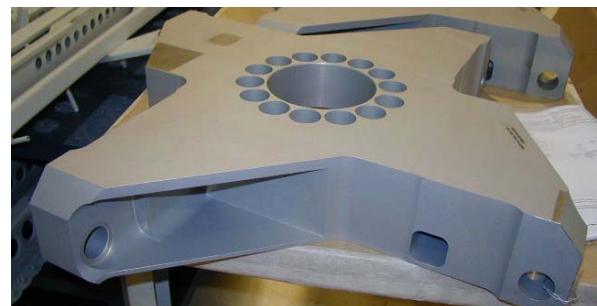


Figure 6: Combiner plate. SPASA photo

Of course, after all manufacturing steps were finished, SPASA quality department performed a final inspection of the parts to ensure the part itself and the documentation fulfils the requirements.

The cuff

Within DART, the blade activity was limited to design with no hardware manufacturing request. Despite this limitation, this was a very important driving factor for the hub design itself because it enabled validation of the major design options. However, this option was considered to be too penalizing in terms of manufacturing difficulties anticipation and tests loading conformity. Therefore, early in the program, the option to actually manufacture a cuff was retained.

The cuff manufacturing followed a specification which was very severe in terms of loads capacity, hub and blade interfaces aerodynamic contour,

environment conditions, planning, costs, and manufacturing constraints.

Contrary to that of helicopters, the tiltrotor blade root generates significant drag at high speed in forward flight. This forces designers to emphasize the cleanliness of the blade root and adopt shapes which generate more difficulties for manufacturing or for substantiation in terms of rigidities and loads capacity.

For costs reasons, the manufacturing process retained for the cuff consisted of stacking carbon and glass pre-preg plies in half moulds. Other processes such as winding, fibre placement, tape layout, RTM were also considered but not retained for costs and schedule reasons, or because they were not suited for these complex parts.

The cuff manufacturing started with the moulds design and manufacturing. It entailed analysis of the plies layout, heat transfer during curing, press system, and demoulding constraints after curing.

Once the moulds were available, the manufacturing started with the cut, stacking and debulking of the pre-preg plies.

Curing was performed in autoclave for the complete cuff in one step.

The manufacturing ended with some limited machining and bushes installation at the cuff interface.

Figure 7 shows the cuff after machining and bushes installation.



Figure 7: The cuff. EC photo

The yoke

The yoke is connected to the mast through the hub spring frame and the homokinetic drive system. It is also connected to the inner and outer pitch bearings.

The yoke contains a thick centre section and four “arms” with flap-wise flexible zones to accommodate static deflections induced by thrust while providing stiff in-plane properties. The yoke and systems connected to it are shown in Figure 8. Within the DART project, NLR was responsible for the manufacture of two yokes, including moulds design.

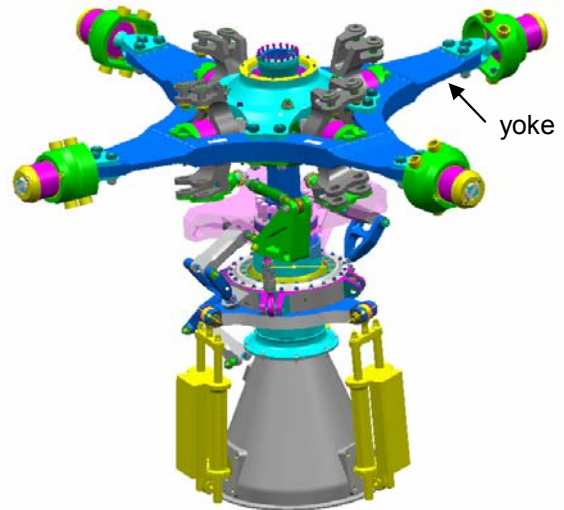


Figure 8: Yoke and surrounding systems

Due to the large number of attachment interfaces and the critical bending stiffness of the yoke, the required dimensional tolerances are very tight. Nowadays, components with tight dimensional tolerances often are manufactured using Resin Transfer Moulding (RTM) with matched metal moulds. However, in case of the yoke an extremely tough resin system is required to fulfil the airworthiness requirements regarding damage tolerance as well as reliability. No commercially available RTM resin system could fulfil these requirements as well as most prepreg materials.

Based on reliable material data and in-service experience from Eurocopter, Hexcel ES18/1055 E-glass prepreg was selected. Potential drawbacks of this system are the exothermal heat development and void formation if the manufacturing process is not mastered; in these adverse conditions, the resin high viscosity in combination with ultra-fast curing during the exothermal peak could result in high void concentrations inside the laminate (typically > 3%).

Classical press curing systems can provide high quality yokes with accurate dimensions for this resin system, but they require a lot of experience to master the process parameters. Therefore, it was decided to develop an alternative manufacturing process that would be more robust. The development

concentrated on press curing using matched metal moulds with oil heating/cooling. This is because press curing can provide the required dimensional tolerances and oil cooling of metal moulds can be very effective during the exothermal peak.

Press curing usually involves the application of heat and pressure on the part, thereby compressing the laminated plies till the required thickness is achieved. In case of ES18/1055 prepreg, this can result in laminates with a high void content due to minimal resin flow and the absence of vacuum. In order to overcome these drawbacks, an alternative process including the application of vacuum was developed.

The temperature window of the process was developed using data from an extensive program involving Differential Scanning Calorimeter (DSC) tests and autoclave manufacturing tests. Next a thermal model was developed and the data of the tests were compared with thermal simulations carried out by CIRA. Based on further simulations the temperature window of [Figure 9](#) was defined.

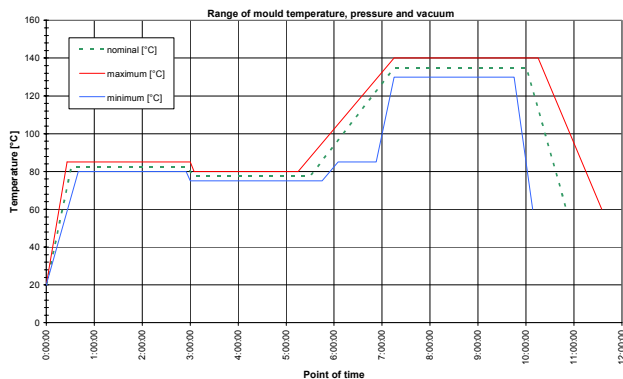


Figure 9: Temperature window of the alternative manufacturing process for ES18/1055 prepreg

The temperature profile shows a long dwell at approximately 80° C. During this dwell the ES18 resin starts to develop exothermal heat and therefore the moulds are cooled to prevent build up of exothermal heat. During the long dwell the moulds are closed slowly, enabling the resin to flow sufficiently. The gradual closing process results in good part quality with a low void content. After a dwell of 300 minutes, the temperature is ramped up to cure temperature. The remaining exothermal peak inside the laminate is sufficiently low because most of the exothermal heat has removed during the dwell. The alternative manufacturing process was validated through the manufacture of 60 mm thick specimens. These specimens showed an excellent quality with very low void content (<0.4%).

The yokes were manufactured at NLR using a matched metal mould consisting of a lower mould with the yoke geometry and a top lid. Both mould parts contained an oil circuit for accurate temperature control. Furthermore the lay-out of the lower mould provided accurate positioning of all plies, see [Figure 10](#) .



Figure 10 : Yoke lower mould during laminating. NLR photo

The top lid was provided with several vents around the circumference of the yoke for the application of vacuum. At the same time these vents were used to remove some excessive resin from the resin-rich prepreg during the closing process. It was decided to use bolts for clamping the mould halves together because no large press was available. Several o-rings were applied in order to be able to apply vacuum before the mould is fully closed.

The process parameters during the cure process were measured using two pressure sensors and several thermocouples. Besides measuring the mould temperatures, also the temperature inside the laminate was measured using sheathed thermocouples at the position of the mounting holes of the hub spring frames and outer pitch bearings.

Both yokes were manufactured successfully using the alternative manufacturing process. Exothermal peak temperatures were within the acceptance limits. The pre-cone angle of the four “arms” with flap-wise flexible zones was very accurate. The thicknesses of the various sections of the yokes were influenced significantly by polymerisation shrinkage of the ES18 resin but the mounting surfaces could be machined to the required dimensions.

After machining the mounting holes were equipped with liner bushes. All bushes were designed with an interference fit and installed after cooling in liquid Nitrogen. One of the finished yokes is shown in [Figure 11](#).



Figure 11: Finished yoke. NLR photo

The finished yokes were inspected using C-scan at CIRA. The second yoke contained some more porosity in the surface plies. Compared to the first yoke the only difference was that the mould was closed slightly faster. Therefore it can be concluded that closing of the mould is the critical step in the yoke manufacturing process. If the mould is closed too fast the viscous ES18 resin will not flow sufficiently and inclusion of volatiles will occur. The use of bolts for closing the mould increased the complexity of the closing/pressing process. The process can be improved and simplified in future through the application of a large press and a number of pressure transducers in the mould to adapt the closing process.

The hub-spring

PAULSTRA long experience in the manufacturing of helicopters laminated bearings made the company an excellent candidate for the design, manufacturing, and testing of the DART elastomeric parts.

For all elastomeric components, the parts design took place in parallel with the tooling design and the process detailed definition.

Several iterations were necessary to insure a correct pressure application on the frames, a correct flow of the elastomeric material during moulding and a satisfactory cooling at the end of the process.

The tooling requirements are very severe in terms of dimensions tolerances, shims positioning and stability during moulding.

PAULSTRA large database in terms of materials helped select the best compromise for the considered application and environmental conditions. This process proved to be effective as all parts could be manufactured correctly at first shot. For example,

the hub spring moulding phase could be performed with no specific difficulties despite the big size of the metallic frames.



Figure 12: Hub spring bearing outer frame. PAULSTRA photo



Figure 13: Hub spring bearing shims. PAULSTRA photo



Figure 14: Hub spring bearing after moulding. PAULSTRA photo



Figure 15: Upper & Lower Hub spring bearings. PAULSTRA photo

The centrifugal force bearing

The centrifugal force bearing manufacturing required a particular attention to the process setting due to the large number of layers.

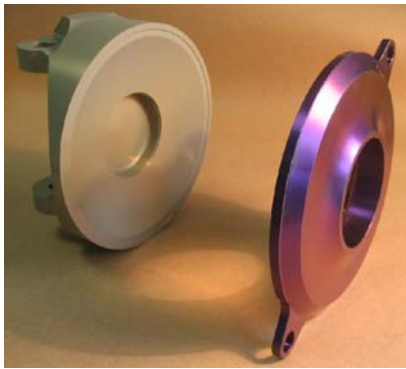


Figure 16: Inner CF bearing. PAULSTRA photo



Figure 17: Inner CF bearing. PAULSTRA photo

A special laminated shape for the laminated part has been defined for buckling stability reasons. This optimisation work has been done by using FEA to estimate the stability of the part, and has been experimentally validate on a dedicated test bench



Figure 18: CF bearing mould components. PAULSTRA photo

The homokinetic drive system bearing

The HDS spherical elastomeric bearings were the first parts moulded in order not to delay the HDS assembly and testing test. No particular difficulties were encountered for this part.



Figure 19: the homokinetic drive system bearing. PAULSTRA photo

Inspection

NDE inspection of the yokes

For the inspection of the yokes, aimed at detecting quality problems such as delamination or high void content, two typical Ultrasonic testing techniques have been used: the Through Transmission (TT) and the Pulse Echo (PE).

The TT test involves the use of two transducers, one acting as transmitter, the other one as receiver. This test allows measurement of the amplitude of the signal passing through the material and, if there are heterogeneities, to detect quality problems.

The PE test is carried out with one 1 MHz plane transducer acting as transmitter and receiver and it is based on the received echoes coming from the interfaces in the material. Not only the amplitude received are measured but also the time (or the space if the velocity is known) spent by the signal to do a round trip. When there are echoes from interfaces between the two surfaces of the material, then they can reveal defects such as inclusions or delaminations.

For both yokes, a preliminary TT test has been performed in order to obtain a global early vision of their compositions. After that, in the zones where possible defects seemed to be present, a deepen test has been carried out via the PE technique.

The following pictures are composed of a histogram and a C-Scan. For the PE result, the colours in the histogram establish a correspondence between the number of points and the distance/thicknesses measured.

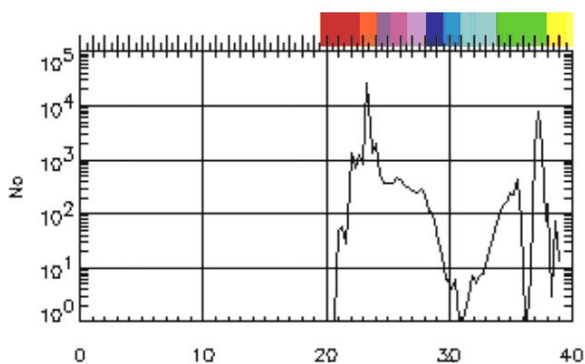


Figure 20: Histogram PE results.

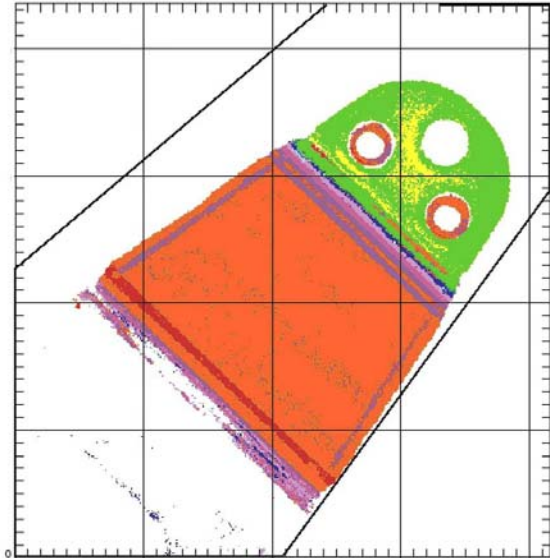


Figure 21: PE results.

These investigations proved to be efficient as minor defects could be detected. Overall, the yoke quality was considered to be particularly good.

Tests

Yoke material samples testing

Two sets of mechanical tests have been performed on the composite samples: three-points bending fatigue tests and four points crack propagation tests.

The first ones were performed on the intact composite samples in a load control mode to evaluate the number of cycle at rupture, while the latter have been performed on composite samples with a cut of depth equivalent to 2 plies all along the width, in a displacement control mode to monitor the crack propagation.

Mechanical tests were executed using a servo-hydraulic equipment, MTS 810 with a 15 KN load cell, calibrated also within the range 0 KN to 3 KN.

No sensors (strain gauges, rosette, etc.) were installed on the sample. The crack propagation was monitored using a dye penetrating liquid introduced in the crack. The tests were performed at room temperature (RT) with dry conditions

The samples were made of Hexcel ES18 resin and a glass fibre woven fabric (type 1055) with 83% weight

fibre in warp direction and the 17% of stitching in the weft direction.

Figure 22 and Figure 23 provide the fatigue and propagation tests schematisation.

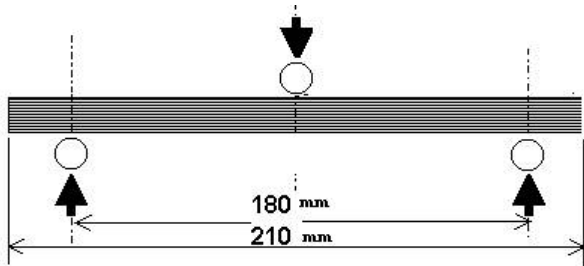


Figure 22: Three-points bending test schematisation

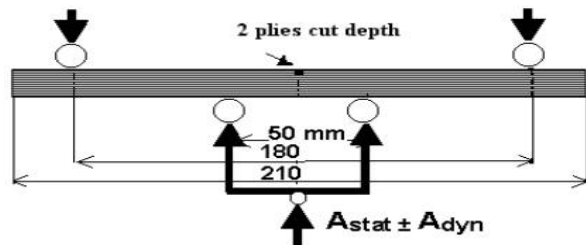


Figure 23: Four-points bending test schematisation

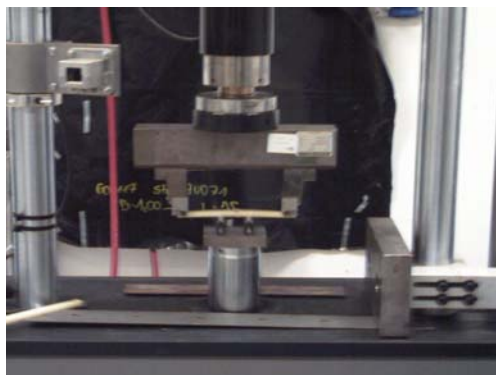


Figure 24: 4-points bending test apparatus. CIRA photo

A preliminary static 3-point bending test was performed to evaluate the ultimate load level and therefore to fix an appropriate static load.

Figure 25 and Figure 26 report the sample at the end of the static test. As expected due to the stacking

sequence of the sample, a typical delamination failure occurred.

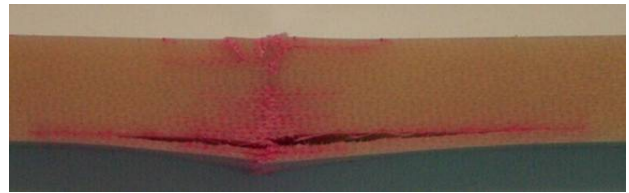


Figure 25: delamination static test. CIRA photo

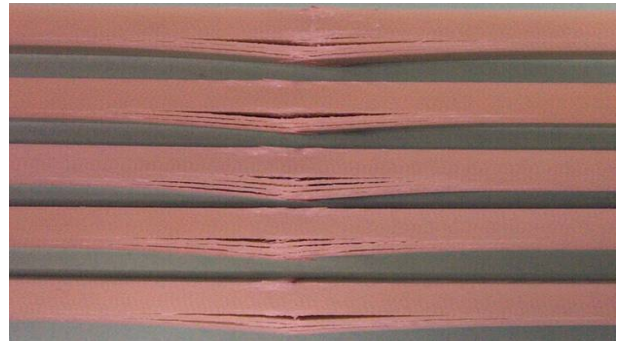


Figure 26: Zoom-in of damaged area. CIRA photo

Crack monitoring during the 4-point bending tests was performed measuring the crack length after pouring a coloured dye penetrating liquid (RACOL dye penetrant) into the cut off. As main lay-up direction of the fibres was at 0°, no crack growth of the V-notch was expected through the thickness. Due to the high tensile stresses experienced at the tip V-notch, delamination occurred gradually reducing the sample stiffness. Crack length evolution as a function of cycle number is reported for all the samples in Figure 27.

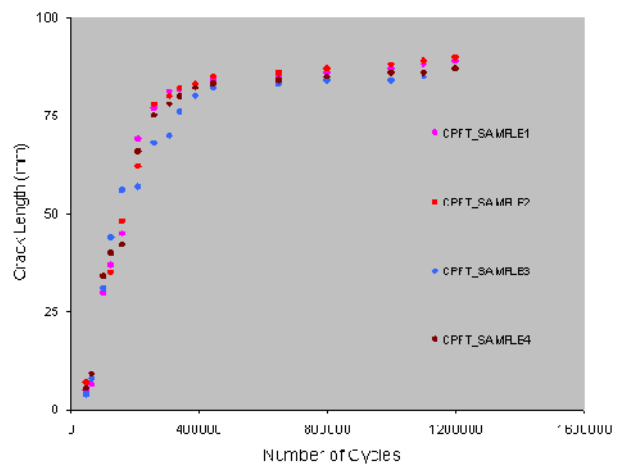


Figure 27: Crack length vs number of cycles for all samples during a 4-points bending fatigue test

Delamination damage is clearly visible thanks to the red dye liquid used to monitor the crack propagation

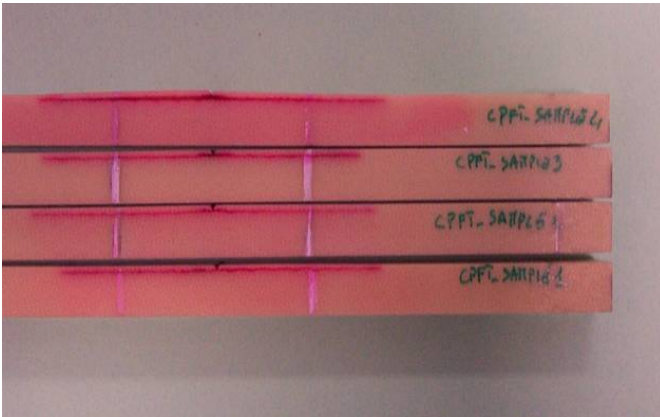


Figure 28: Side view of the sample crack at the end of fatigue test in 4-point bending mode. CIRA photo

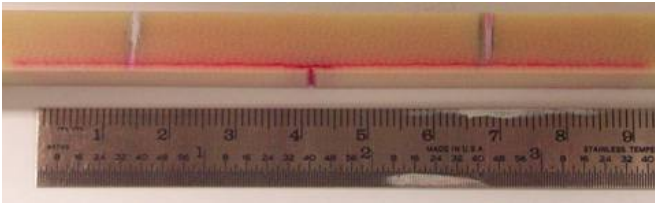


Figure 29: Crack length after 1.200.00 cycles. CIRA photo

Hub-spring testing

The fatigue behaviour of the hub spring elastomeric bearings is critical for the rotor performance. This part reacts the blades thrust and in-plane forces that are transmitted by the blades. It also accommodates hub tilting at large angles. In the rotating frame, this translates in alternate cocking motions at the rotor rotating frequency.

Another very important characteristic of the part is its self heating property, which has to be kept minimal for reliability reasons. Additionally, attention has to be paid to the heat transfer from the elastomer to the environment.

To qualify the hub-spring, a dedicated fatigue test bench has been developed by PAULSTRA. It allows the application of the static thrust and the dynamic cocking motion of the bearings. A general view of the bench is presented in [Figure 30](#).



Figure 30: PAULSTRA hub spring bench. PAULSTRA photo

Centrifugal force bearing testing

The centrifugal force bearing presents very specific challenges in terms of number of shims, low thickness, high loads and large amplitudes. For the buckling stability assessment, the part was tested on a 6 axis bench.

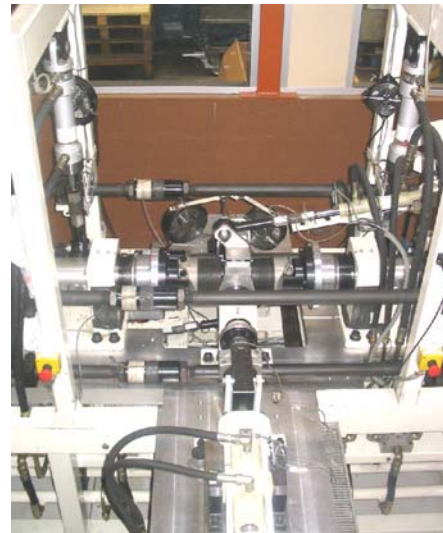


Figure 31: PAULSTRA 6 axes bench. PAULSTRA photo

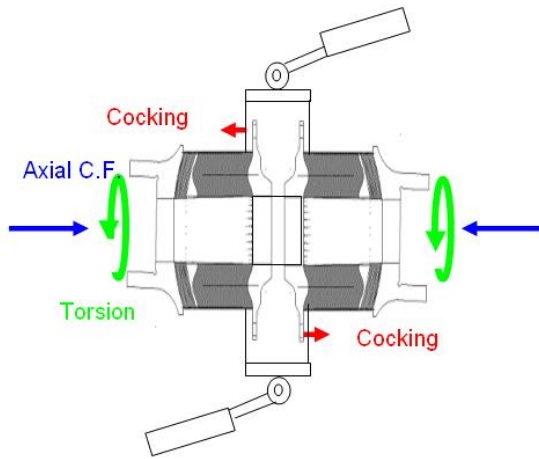


Figure 32: PAULSTRA 6 axes bench scheme

The application of the centrifugal force in combination with pitch torsion and cocking motion did not highlight any instability.



Figure 33: 44° Torsion of CF bearing. PAULSTRA photo



Figure 34: 3° cocking on CF bearing. PAULSTRA photo

Spindle testing

The spindle transmits the blade and cuff centrifugal force through the half cones at the elastomeric pitch bearing interface. It also transmits the cuff in-plane and out-of plane loads to the yoke through the journal pitch elastomeric bearing (see [Figure 35](#)).

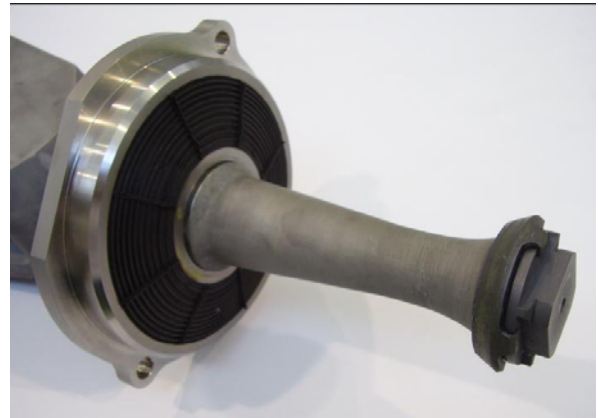


Figure 35: the spindle. EC photo

The spindle test objectives were:

- to check the behaviour of the spindle attachment on the dummy yoke
- to check the behaviour of the spindle and half thrust cone assembly loaded by external forces and moments.

The forces represent the blade centrifugal force and the moments represent the cocking moments transmitted by the centrifugal force bearing as a consequence of the yoke coning motion.

The spindle was installed on a dummy yoke on one side and a beam interfacing the half thrust cones conical areas on the other side. At the beam ends, 2 actuators were installed to load the assembly, simulating the centrifugal force and the moments due to the yoke coning.

Strain gauges were installed on test bench at 2 stations to measure the moments on the dummy yoke and at the bench interface.

2 laser beams measured the relative displacements between the dummy yoke and the beam. They represent both the displacements due to the spindle-dummy yoke attachment and the displacements due to the conical interfaces between the spindle and the beam.

2 laser beams measured the relative displacements between the spindle and the beam. They represent only the displacements due to the conical interfaces between the spindle and the beam

Laser beams were located at both sides of the beam and measurements combined to estimate both the displacement and the rotation of the beam.

The spindle was equipped with strain gauges to assess the traction and the bending moments generated by the actuators. 4 strain gauges were installed close to the conical interface with the half thrust cones as presented in figure 1.

Springs were set between the beam and the actuators bodies in order to pre-load the assembly.

Figure 36 provides a scheme of the spindle test bench.

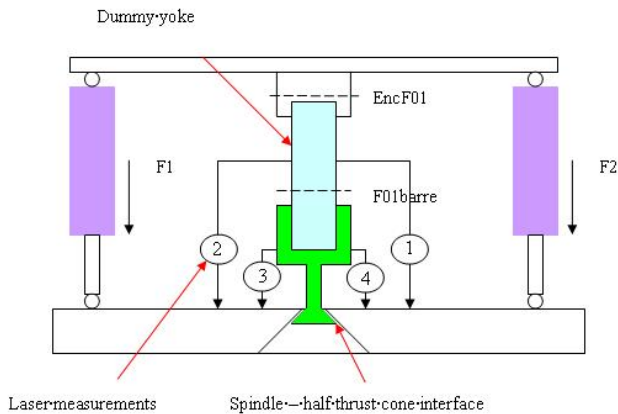


Figure 36: spindle test bench scheme

The spindle test was performed up to a maximum CF loading of 45 tons, which covers 115% of the RPM of the theoretical nominal centrifugal force of 34 tons (see Figure 37).

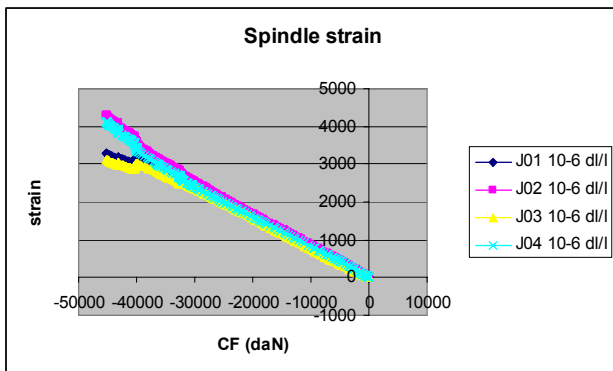


Figure 37: spindle test bench

No damage was observed on the parts and the analysis of the rigidity of the spindle interfaces did not reveal any particular problem along the traction axis.

Homokinetic drive system testing

The homokinetic drive system (see Figure 38) is made of an inner flange driving 2 outer flanges to which 2 sets of 2 drive links are connected.

In the DART hub, the other drive link ends interface with the hub spring.

A more detailed description of the system can be found in reference [21].

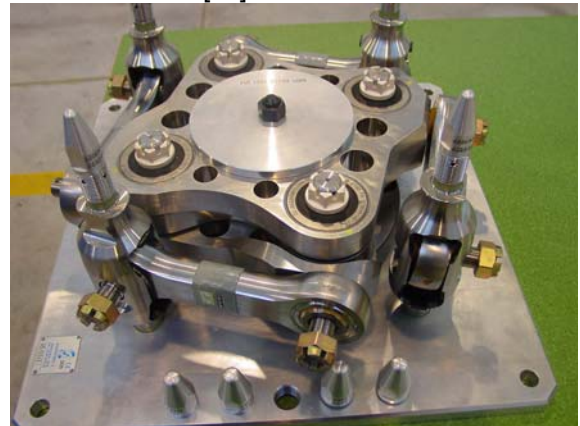


Figure 38: the homokinetic drive system. EC photo

For its testing, the homokinetic drive system is installed on a dummy hub made of two plates, which spherical interfaces enable the hub tilting. Around the mast, 2 spacers with spherical boundaries interface with the dummy hub.

On the test bench (see Figure 40), the dummy hub interfaces with 2 beams that are linked through dry journal bearing to vertical rods. These rods force the hub tilt along one axis. They enable in-plane motions and react vertical loads and moments along the axis normal to the tilting axis.

The hub interfaces with 2 additional beams that are connected through 2 dry bearings to 2 actuators. These actuators force the hub tilt and are displacement controlled. The beams are also connected to cables that are used to load the system, both in terms of torque and in terms of in-plane loads. This is achieved thanks to 2 horizontally disposed actuators.

Strain gauges are installed on the drive links to measure traction, and on the vertical rods to measure the rods reactions. Strain gauges are also

installed on the mast to measure torque and bending moments along 2 axes and at two different stations.

2 displacement transducers measure the absolute displacements of the hub at the torque and in-plane loading points.

2 additional displacement transducers measure the absolute displacements of the hub at the tilting actuators interfaces.

Figure 39 presents the bench scheme. The tilting motion is imposed by actuators 1 and 2. Displacement transducers measure the displacements at the loading points of the vertical actuators in order to control the magnitude of the hub tilt. Moments on the mast are measured around 2 azimuths at 2 different stations:

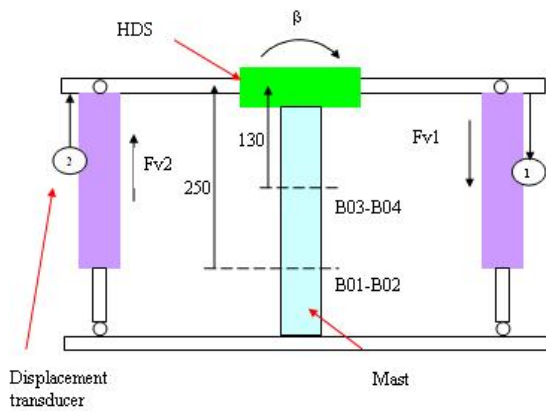


Figure 39: test bench tilting scheme



Figure 40: test bench overview. EC photo

The test enabled the validation of the correct performance of the homokinetic drive system.

One of the most interesting features of the homokinetic drive system is its equivalent stiffness matrix at the rotor hub. This matrix relates tilting moments to tilting rotations. This is 2 by 2 matrix.

The aim of the test was also to check this equivalent stiffness. Tilting is forced along one axis and moments are measured along 2 axis. The moment reacted along the tilting axis is called in-phase moment, while the other one is called out of phase moment.

Figure 41 presents the comparison of measured and predicted in phase bending moments at the rotor hub. One can notice a very good correlation between the two curves.

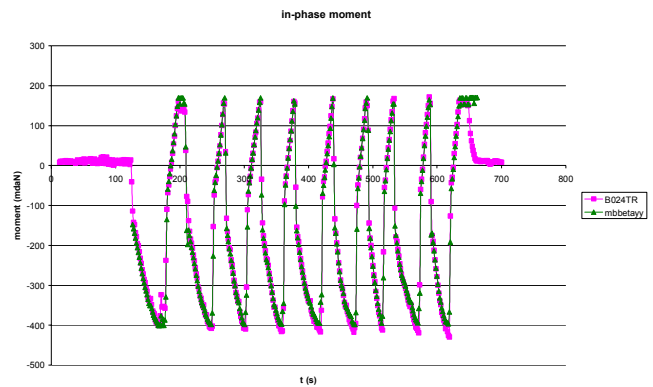


Figure 41: in-phase bending moment

Figure 42 presents the comparison of measured and predicted out of phase bending moments at the rotor hub. One can also notice a very good correlation between the two curves.

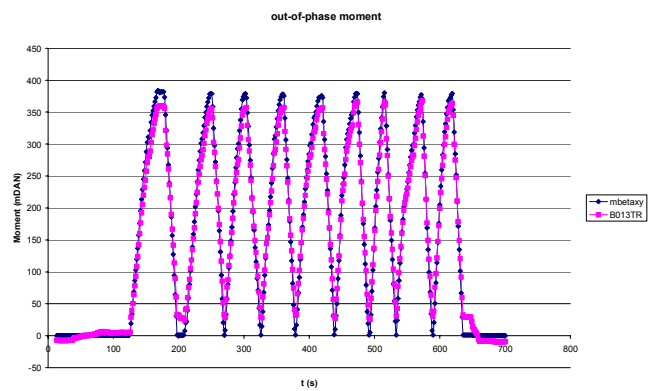


Figure 42: out of phase bending moment

The hub testing

The hub static testing is aimed at checking the quasi static behaviour of the hub, both in terms of rigidity and loads transfer and sharing.

The following picture presents the DART yoke in the static test bench. The tests started end of May and should be completed end of June.



Figure 43: static test bench. EC photo

Conclusions

The DART program has now completed the manufacturing phase and is entering into the final phase of the test program.

The manufacturing phase was successful as all parts were manufactured in due time according to specification with minor and very limited repairs.

The metallic parts manufacturing was organised with a very tight planning in order to deliver parts in time for testing or for moulding elastomeric parts.

The elastomeric components were manufactured with very limited iterations in very short time-frame. Characteristics at first shot were very close to specifications. The buckling test of the centrifugal force bearing was successful.

Two very challenging composite parts, the yoke and the cuff were manufactured with high quality in a very short time schedule. For the yoke, an alternative manufacturing process was proposed. The curing cycles were optimised through DSC analysis, and samples manufacturing and fatigue testing.

All tests completed up to now were successful and no major problem was encountered.

The program is now close to its end with the final static test to be completed end of June 2006.

DART consortium

AGUSTA
CIRA
EUROCOPTER
EUROCOPTER DEUTSCHLAND
NLR
ONERA
PAULSTRA
SENER
SPASA
WESTLAND

Acknowledgements

The authors would like to express their gratitude and esteem to the partners involved in the DART program for their very fruitful contribution and co-operative and open-minded attitude.

Gratitude is also expressed to the European Commission who has sponsored this program and encouraged this co-operation among European helicopter manufacturers, suppliers and design and research centres.

References

- [1] Thomas Müller, Michael Hirschberg, Alexis Rocher, "French Low-speed V/STOL concepts of the twentieth century", AHS Forum 58, Montreal, Quebec, Canada, June 11th 2002
- [2] Thomas Müller, Michael Hirschberg "German V/STOL rotorcraft and propellercraft in the twentieth century", AHS Forum 57, May 9-11th 2001
- [3] Michael Hirschberg, Thomas Müller, Erasmo Piñero "Italian V/STOL STOL concepts of the twentieth century", AHS Forum 59, Phoenix, Arizona May 6-8th 2003
- [4] F. Beroul, P. Bassez, P. Gardarein, "EUROFAR dynamic test", .18th ERF, Avignon, 15-18 Sept 92.
- [5] V.Caramaschi, G.Maffioli, "Design and Manufacturing Concepts of Eurofar Model#2 Blades",AHS 48th Annual Forum, Washington D.C. June 3-5th 1992
- [6] F. Nannoni, G. Giancamilli, M. Cicalè "ERICA: the European advanced Tiltrotor", 27th European Rotorcraft Forum, Moscow, Russia, 11-14th September 2001
- [7] M. Cicalè, F. Nannoni, A. Pisoni, M. Allongue, P. Rollet, P. Hellio, - "The Aerodynamic Challenge Of The European Advanced Tiltrotor", CEAS Aerospace Aerodynamics Research Conference – 10-13th June 2002 – Cambridge, United Kingdom
- [8] P. Alli, F. Nannoni, M. Cicalè, "Erica: The European Tiltrotor Design And Critical Technology Projects", Presented at AIAA/ICAS International Air and Space Symposium and Exposition. Dayton, 14-17th July 2003
- [9] C.Bottasso,L.Trainelli, P.Abdel Nour, G.Labò, "Tilt rotor analysis and design using finite-element multibody procedures", 28th ERF Bristol, UK, 17-20th September 2002
- [10] M. W. Nixon, C., W. Langston, J. D. Singleton, D. J. Piatak, R. G. Kvaternik, L. M. Corso, R. Brown, "Aeroelastic stability of a soft-in-plane gimballed tilt-rotor model in hover", .42nd AIAA/ASME/ASCE/AHS/ASC Structures, Structural dynamics and materials conference, Seattle, Washington, April 16-19, 2001.
- [11] B. Manimala, G. Padfield, D. Walker, M. Naddei, L. Verde, U. Ciniglio, P. Rollet, F. Sandri , "Load alleviation in tilt-rotor aircraft through active control: modelling and control concepts", AHS Forum 59, Phoenix, Arizona, May 2003.
- [12] C.W. Acree, Jr, "Rotor design options for improving V-22 whirl-mode stability", AHS Forum 58, Montreal, Quebec, Canada, June 11-13th 2002
- [13] W. Johnson, "Technology drivers in the development of CAMRAD II", Johnson Aeronautics, Aeromechanics Specialists Conference, San Francisco, 1994
- [14] W. Johnson, "Tiltrotor aeromechanics", April 1987
- [15] W.G. Sonneborn, E.O. Kaiser, C.E. Covington and K. Wilson, "V22 propulsion system design".
- [16] C.W. Acree, Jr, R.J. Peyran, W. Johnson, "Improving tilt-rotor whirl-mode stability with rotor design variations", 26th ERF, The Hague, Netherlands, Sept.26-29, 2000.
- [17] T. Parham, Jr., L.M. Corso, "aeroelastic and aeroservoelastic stability of the BA609".
- [18] J.L. Potter "The application of Elastomeric products on the V22 tilt-rotor aircraft", Lord Corporation, Amsterdam, September 12-15-1989
- [19] M.K. Farrell, "Aerodynamic design of the V22 Osprey proprotor, Boston, May 22-24,1989.
- [20] B. Benoit et al. , "HOST, a General Helicopter Simulation Tool for Germany and France", AHS Forum 56, Phoenix, Virginia, May 2000.
- [21] E. Zoppitelli et al. , "DART: development of an advanced rotor for tilt-rotor", ERF Forum 30, Marseille, France, Sept-2004.